

250 years Lambert surface: does it really exist?

Alwin Kienle* and Florian Foschum

Institut für Lasertechnologien in der Medizin und Meßtechnik, Helmholtzstr.12, D-89081 Ulm, Germany

*alwin.kienle@ilm.uni-ulm.de

Abstract: The time-honored Lambert law is widely applied for describing the angle resolved reflectance from illuminated turbid media. We show that this law is only exactly fulfilled for a very special set of geometrical and optical properties. In contrast to what is believed so far, we demonstrate theoretically and experimentally that huge deviations from the Lambert law are ubiquitous. This finding is important for many applications such as those in biomedical optics.

© 2011 Optical Society of America

OCIS codes: (170.3660) Light propagation in tissue; (290.0290) Scattering; (290.1990) Diffusion; (290.7050) Turbid media.

References and links

1. J. H. Lambert, *Photometria sive de mensura et gradibus luminis, colorum et umbrae* (Eberhard Klett, 1760).
2. H. Gross, *Handbook of Optical Systems; Volume 1: Fundamental of Technical Optics* (Wiley-VCH, 2005).
3. S. Georgiades, P. N. Belhumeur, and D. J. Kriegman, "From few to many: illumination cone models for face recognition under variable lighting and pose," *IEEE Trans. Pattern Anal. Mach. Intell.* **23**, 243–260 (2001).
4. M. S. Patterson, B. Chance, and B. C. Wilson, "Time-resolved reflectance and transmittance for the noninvasive measurement of tissue optical properties," *Appl. Opt.* **28**, 2331–2336 (1989).
5. A. Kienle, L. Lilge, M. S. Patterson, R. Hibst, R. Steiner, and B. C. Wilson, "Spatially-resolved absolute diffuse reflectance measurements for non-invasive determination of the optical scattering and absorption coefficients of biological tissue," *Appl. Opt.* **35**, 2304–2314 (1996).
6. F. Martelli, S. Del Bianco, A. Ismaelli, and G. Zaccanti, *Light propagation through biological tissue and other diffusive media: theory, solutions, and software* (SPIE Press Book, 2009).
7. D. J. Durian, "Influence of boundary reflection and refraction on diffusive photon transport," *Phys. Rev. E* **2**, 857–865 (1994).
8. S. C. Gebhart, A. Mahadevan-Jansen, and W.-C. Lin, "Experimental and simulated angular profiles of fluorescence and diffuse reflectance emission from turbid media," *Appl. Opt.* **44**, 4884–4901 (2005).
9. D. C. Adler, Y. Chen, R. Huber, J. Schmitt, J. Connolly, and J. G. Fujimoto, "Three-dimensional endomicroscopy using optical coherence tomography," *Nature Photon.* **1**, 709–716 (2007).
10. V. Backman, M. B. Wallace, L. T. Perelman, J. T. Arendt, R. S. Gurjar, M. G. Müller, Q. Zhang, G. Zonios, E. Kline, T. McGilgan, S. Shapshay, T. Valdez, K. Badizadegan, J. M. Crawford, M. Fitzmaurice, S. Kabani, H. S. Levin, M. Seiler, R. R. Dasari, I. Itzkan, J. Van Dam, and M. S. Feld: "Detection of preinvasive cancer cells," *Nature* **406**, 35–36 (2000).
11. J. Xia and G. Yao, "Angular distribution of diffuse reflectance in biological tissue," *Appl. Opt.* **46**, 6552–6560 (2007).
12. R. Michels, F. Foschum, and A. Kienle, "Optical properties of fat emulsions," *Opt. Express* **16**, 5907–5925 (2008).
13. F. Martelli and G. Zaccanti, "Calibration of scattering and absorption properties of a liquid diffusive medium at NIR wavelengths. CW method," *Opt. Express* **15**, 486–500 (2007).
14. R. Graaff, J. G. Arnoudse, F. F. M. de Mul, and H. W. Jentink, "Similarity relations for anisotropic scattering in absorbing media," *Opt. Eng.* **32**, 244–252 (1993).
15. D. C. Van der Hulst, *Multiple Light Scattering* (Academic Press, 1980).
16. A. Kienle, C. D'Andrea, F. Foschum, P. Taroni, and A. Pifferi, "Light propagation in dry and wet soft wood," *Opt. Express* **16**, 9895–9906 (2008).

17. A. Kienle and R. Hibst, "Light guiding in biological tissue due to scattering," *Phys. Rev. Lett.* **97**, 018104 (2006).
18. H. A. Yousif and E. Boutros, "A FORTRAN code for the scattering of EM plane waves by an infinitely long cylinder at oblique incidence," *Comput. Phys. Commun.* **69**, 406–414 (1992).
19. Y. Sun, "Statistical ray method for deriving reflection models of rough surfaces," *J. Opt. Soc. Am. A* **24**, 724–744 (2007).
20. P. Beckmann, A. Spizzichino, and A. Norwood, *The Scattering of Electromagnetic Waves from Rough Surfaces* (Artech House, Inc., 1987).
21. A. Ishimaru, *Wave Propagation and Scattering in Random Media* (Academic Press, 1978).
22. M. I. Mishchenko, L. D. Travis, and A. A. Lacis, *Multiple Scattering of Light by Particles: Radiative Transfer and Coherent Backscattering* (Cambridge U. Press, 2006).
23. F. Voit, J. Schäfer, and A. Kienle, "Light scattering by multiple wpheres: comparison between Maxwell theory and radiative-transfer-theory calculations," *Opt. Lett.* **34**, 2593–2595 (2009).

1. Introduction

The concept of Lambert surface - a surface having a cosine-dependent reflectance (radiant intensity) versus polar angle - was presented 250 years ago [1] and is now often used in many research fields, especially in photonics, e.g. in optics design [2], in computer graphics [3], and in biomedical optics [4–6]. However, it is, in general, not known how good this Lambert law is fulfilled for illuminated turbid media nor if exact Lambert surfaces exist at all. In literature it was found by applying diffusion theory [7] and Monte Carlo simulations [8] that the Lambert law is approximately correct when the total reflectance is considered. Here, the term 'total reflectance' means that the photons emitted at a certain angle are integrated over all reflectance locations.

In this study we show that for a specific illumination and a specific set of optical properties of a turbid medium the total reflectance is exactly Lambertian. For these investigations it is assumed that the turbid media are semi-infinitely extended and have a plane surface. Turbid media with rough surfaces are outlined in the discussion chapter.

On the other hand, we found that for many relevant applications the Lambert law is completely wrong. It is demonstrated that large deviations from the Lambert law are obtained when not only the polar dependence (averaged over all azimuthal angles) but also the azimuthal dependence of reflectance is considered, especially, at positions close to an incident point beam which is important for early diagnosis of cancer [9, 10]. In general, the azimuthal dependence has been neglected for many applications described in literature apart from studies which considered the reflectance for a small number of azimuthal angles [8, 11].

Finally, we show theoretically and experimentally, using wood as example, that even the total reflectance has large deviations from the Lambert law in turbid media with an aligned microstructure.

2. Methods

The Monte Carlo method was applied to calculate the light propagation in turbid media. Monte Carlo simulations are an exact solution of the radiative transfer equation provided that an infinitely large number of photons are used in the calculations [6]. The radiative transfer theory is usually considered as the gold standard for describing the light propagation in random media, see discussion chapter. In the radiative transfer theory the following quantities are used to describe the optical properties of turbid media: the absorption coefficient μ_a , the scattering coefficient μ_s , the phase function p , often characterized by the anisotropy factor g , which equals the average cosine of the scattering angle, and the refractive index n [6]. At the boundary the probability for reflection and transmission is calculated via Fresnel's formulas.

The results obtained from the Monte Carlo simulations were compared with experiments using a home-built goniometer, with which it is possible to measure almost the whole reflectance

half sphere [12]. The setup for measuring the angle resolved reflectance was verified with experiments using Intralipid. Intralipid is an often used liquid tissue phantom having well known scattering properties, whereas ink served as an absorber [12,13]. The emitted intensity was calibrated with measurements on a reflection standard with known total reflectance. Thus, absolute measurements could be performed.

3. Results

3.1. Reflectance versus polar angle

First, we considered the total reflectance versus polar angle $R(\theta)$ and assumed a turbid medium with randomly aligned microstructure. We systematically investigated the dependence of $R(\theta)$ on the optical and geometrical parameters and found that an exact Lambert surface is obtained for the following conditions: a) the albedo $a = \mu_s / (\mu_s + \mu_a)$ equals 1, i.e. the scattering coefficient is infinitely larger than the absorption coefficient, b) the refractive index is the same inside and outside the turbid medium, c) the angular dependence of the incident light power is $\propto \cos(\theta)$. Figure 1 shows $R(\theta)$ divided by $\cos(\theta)$ using these three conditions for an isotropic phase function (black curve). We note that the beam profile including the beam diameter does not influence the results because the total reflectance is considered. Within the statistics of the Monte Carlo simulations the reflectance is 1 for all θ -angles. We calculated $R(\theta)/\cos(\theta)$ for different phase functions [14], e.g. for high anisotropy values ($g > 0.9$) or obtained from Mie theory, using the three conditions and found that the Lambert law was always valid. For the special case of isotropic scattering and for specific polar angles the result can be validated with data from the literature [15]. In Fig. 1 $R(\theta)/\cos(\theta)$ is also shown for a Henyey-Greenstein phase function with an anisotropy factor of $g = 0.5$ (red curve).

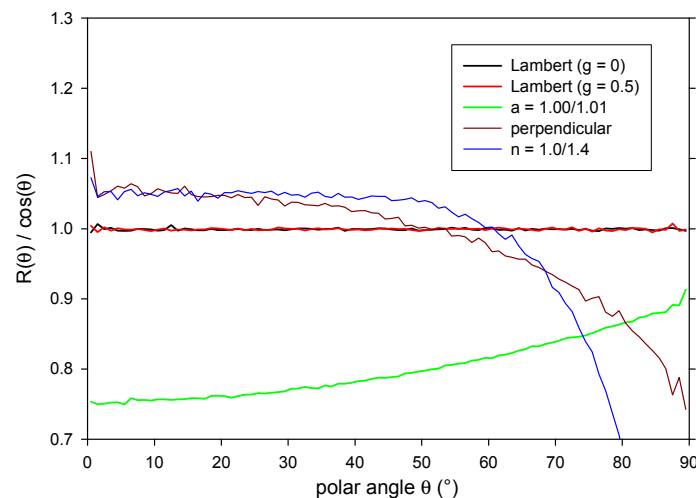


Fig. 1. Monte Carlo simulations for total reflectance versus polar angle ($R(\theta)/\cos(\theta)$) are shown which were calculated for the special set of optical and geometrical parameters to obtain a Lambert surface (black and red curves) and calculated by varying one of these parameters as indicated in the legend.

Next, one of the three conditions for the Lambert law to be valid was altered keeping the others constant. Figure 1 shows $R(\theta)/\cos(\theta)$ for $a = 1/1.01$ (green curve; i.e. with a non-zero absorption coefficient), for perpendicular incident light (brown curve), and for a mismatch of the refractive indices ($n = 1.0$ outside and $n = 1.4$ in the turbid medium, blue curve). A finite

absorption coefficient of the turbid medium results in a smaller reflectance at all angles. The decrease is smaller for large polar angles indicating that the photons emitted at these angles travel a shorter path through the scattering medium, which results in a lower probability for absorption. In principle, the smaller the depth of a considered photon the higher the probability for emission without further scattering interaction and, thus, the higher the relative probability for reflectance at large polar angles. This is caused by the fact that for a photon which is located deeper in the scattering medium the probability for being emitted from the medium at large polar angles (without further scattering) is decreased more than at small polar angles due to the exponential dependence on the photon path.

For perpendicular incident light and for a mismatch of the refractive index $R(\theta)/\cos(\theta)$ decreases for larger polar angles (compare Fig. 1) due to the deeper light penetration (i.e. the longer paths in the turbid medium) and the Fresnel-reflection, respectively. Thus, any alteration of the three conditions results in a non-Lambertian reflectance.

Further, we show the dependence of $R(\theta)/\cos(\theta)$ on the distance to an incident continuous wave point beam having an infinitely small diameter ($\delta(r)$, Fig. 2a) and on the time after an incident pulsed beam having an infinitely small pulse duration ($\delta(t)$, Fig. 2b) by applying the Monte Carlo method. We employed the three standard conditions for obtaining the Lambert surface using $\mu'_s = 1 \text{ mm}^{-1}$ and applied an isotropic phase function. The refractive index inside and outside the scattering medium was 1.4. $R(\theta)/\cos(\theta)$ -curves at three different distance ranges to the incident point beam exhibit significant differences, see Fig. 2a. The penetration depth of photons that are emitted at short distances are smaller compared to the photons that are emitted at large distances. Thus, for the latter case more photons are emitted at smaller angles, see Fig. 1.

A similar behavior as for the spatially resolved reflectance is obtained for the time resolved reflectance, see Fig. 2b. Here the reflectance at a certain time after the incident pulse is summed up for all spatial locations. The penetration depth of photons emitted at short times is smaller than that of photons emitted at long times. Thus, at large angles $R(\theta)/\cos(\theta)$ is increased for short times and is decreased at long times.

3.2. Reflectance versus polar and azimuthal angles

For the results discussed so far the reflectance was presented versus the polar angle, i.e. for each polar angle the reflectance values at all azimuthal angles ϕ were summed up. It could be seen that, when the above mentioned three conditions are not fulfilled, the assumption of a Lambertian surface is incorrect, but the deviations might be tolerable in some situations. However, in many applications the dependence of the emitted light on the polar and on the azimuthal angles $R(\theta, \phi)$ is important. Figure 3 shows $R(\theta, \phi)$ for three positions having different distances from the incident point beam. Reflectance data for the whole reflectance half sphere ($0^\circ \leq \theta \leq 90^\circ$, $0^\circ \leq \phi \leq 360^\circ$) are depicted. Note that for the polar plots the reflectance is not divided by $\cos(\theta)$. The optical properties of the turbid medium were $\mu'_s = 1 \text{ mm}^{-1}$, $\mu_a = 0.001 \text{ mm}^{-1}$ using an isotropic phase function. A perpendicular incident continuous wave point beam and refractive index matching was assumed. The figures show that $R(\theta, \phi)$ is very different from that of a Lambertian surface. At small distances almost all light is emitted in one ϕ -direction ($\phi = 180^\circ$). This is caused by single scattering, which is dominant at small distances, because the single scattered light can only be emitted at $\phi = 180^\circ$ due to geometrical constraints, compare Fig. 3b. For larger distances $R(\theta, \phi)$ becomes more rotationally symmetric (Fig. 3c) which is caused by multiple scattered photons. However, even at a distance of 4.9 mm the reflectance is still anisotropic, compare Fig. 3d. We note that considering only the θ -dependence the reflectance is much closer to the Lambert law for all three distances due to the summing up of reflectance values for the ϕ -angles.

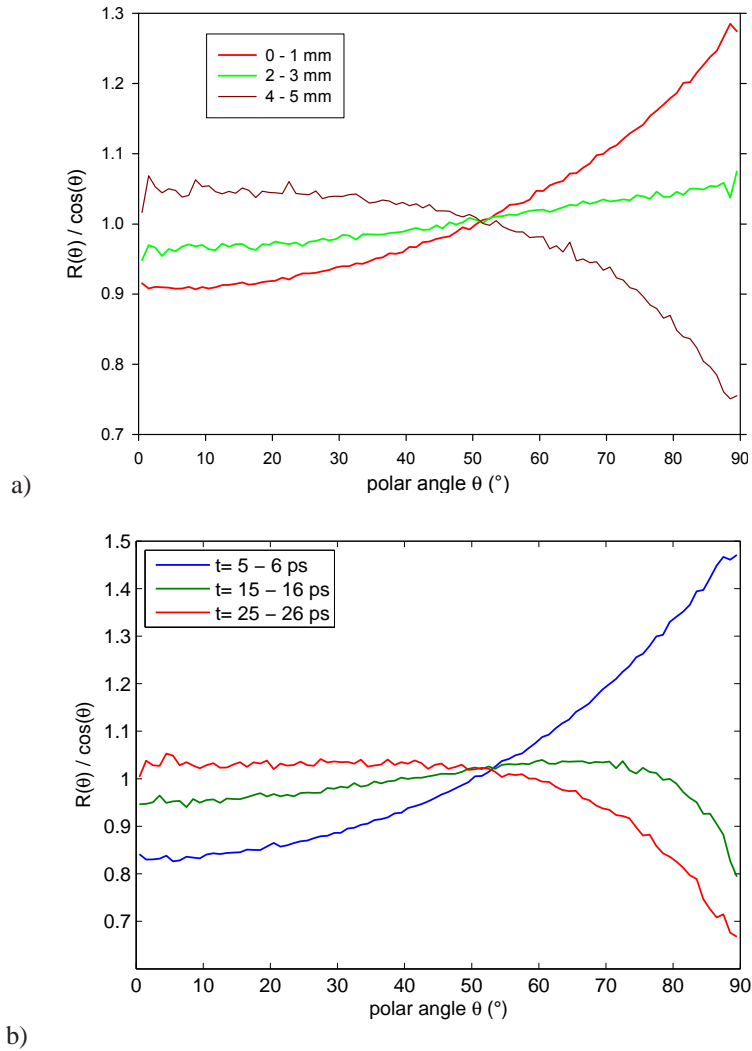


Fig. 2. Reflectance for different distances to the incident source and for different times after the incident pulse calculated with the Monte Carlo method using $\mu'_s = 1 \text{ mm}^{-1}$. a) $R(\theta)/\cos(\theta)$ is shown for a $\delta(r)$ -source and following distance ranges: 0 – 1 mm (red curve), 2 – 3 mm (green curve), and 4 – 5 mm (brown curve). b) $R(\theta)/\cos(\theta)$ is shown for a $\delta(t)$ -source and following time intervals: 5 – 6 ps (blue curve), 15 – 16 ps (green curve), 25 – 26 ps (red curve).

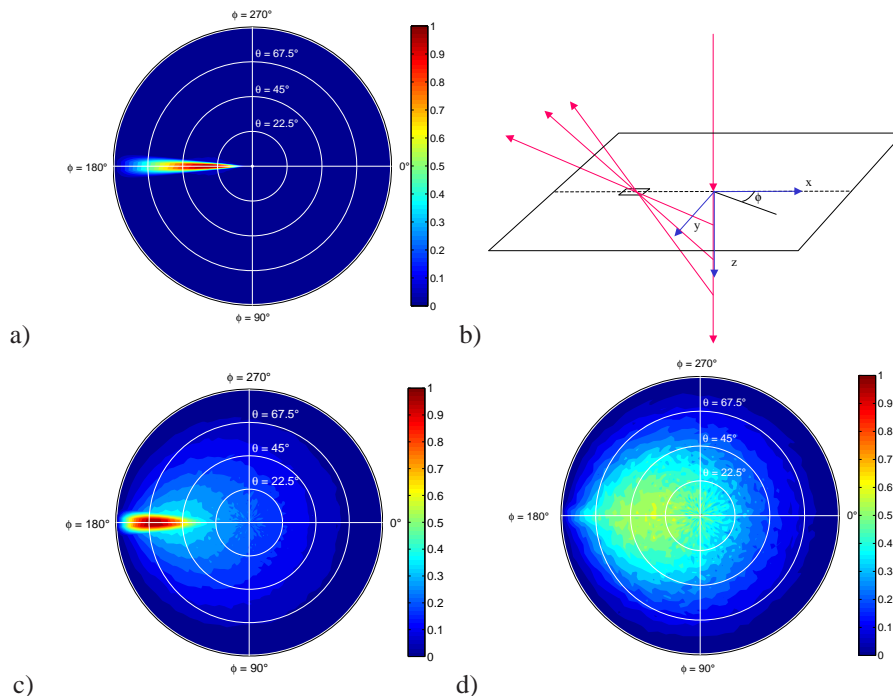


Fig. 3. Reflectance versus polar and azimuthal angles for different positions relative to the incident source. $R(\theta, \phi)$ is shown at a) $x = -0.3 \pm 0.1$ mm, $y = 0$ mm; c) $x = -1.9 \pm 0.1$ mm, $y = 0$ mm; d) $x = -4.9 \pm 0.1$ mm, $y = 0$ mm; b) Scheme of single scattering.

The theoretical results were compared with goniometric measurements. Figure 4 shows experiments on quasi semi-infinitely large Intralipid/ink solutions, which were compared to Monte Carlo simulations. It can be seen that the Monte Carlo simulations agree well with the measurements for all three samples. Note that no parameters were fitted. The decrease of $R(\theta)/\cos(\theta)$ for large polar angles is mainly due to the refractive index mismatch between Intralipid ($n \approx 1.33$) and air ($n = 1.0$), compare Fig. 1.

3.3. Reflectance from turbid media with anisotropic light propagation

In the simulations shown above the turbid media were assumed to exhibit an isotropic light propagation, i.e. the optical properties do not depend on the photons' directions. This is almost always supposed in literature, although many turbid media have an aligned microstructure which causes an anisotropic light propagation. Examples for biological media are muscle, tendon, ligaments, skin, enamel, dentin, or wood. Figure 5 shows a simulation and measurement of $R(\theta, \phi)$ for soft wood. For the simulations we used a model for describing the anisotropic light propagation in wood that we have recently developed [16, 17], see Fig. 5a.

The aligned microstructure of soft wood in growth direction (tracheids) was approximated by infinitely long cylinders with a typical tracheid diameter ($d = 30 \mu\text{m}$, filled with air, see Fig. 5a). The phase functions and the scattering coefficients for the different incident angles relative to the cylinder axis were calculated with an analytical solution of the Maxwell equations [18] and stored for use in the Monte Carlo program [16]. In addition, the contribution of all other scatterers was described by a Henyey-Greenstein phase function ($g = 0.9$). Originally, we used this model to describe the spatially resolved reflectance and compared it successfully

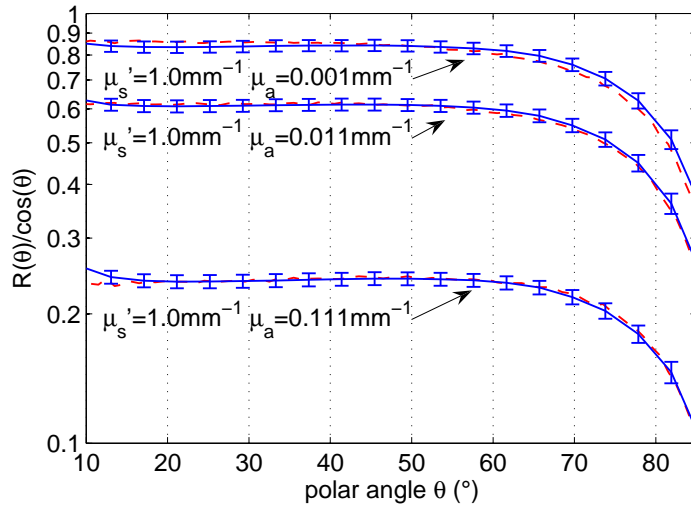


Fig. 4. Measurements (blue solid curves) and Monte Carlo simulations (red dashed curves) of the total reflectance from Intralipid solutions. $R(\theta)/\cos(\theta)$ versus polar angle is shown for three solutions with different amounts of ink and for perpendicular incident light at a wavelength of 640nm. The optical coefficients of the solutions are indicated in the figure.

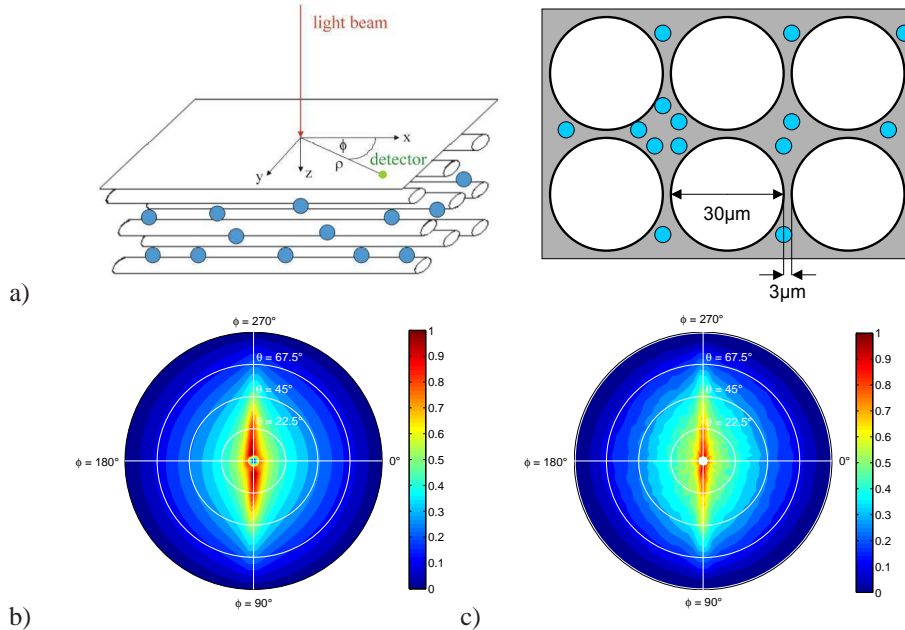


Fig. 5. Angular resolved total reflectance from soft wood. a) Model used for the Monte Carlo simulations (left); Cross section (y, z -plane) of the model (right); b) $R(\theta, \phi)$ obtained from the Monte Carlo simulations; c) $R(\theta, \phi)$ measured on a (optically semi-infinite) soft-wood sample at a wavelength of 640 nm.

to measurements [16]. Here, we took the model and calculated $R(\theta, \phi)$ for the reflectance, see Fig. 5b. A strong anisotropic $R(\theta, \phi)$ is obtained from the Monte Carlo simulations which is mainly due to the scattering characteristics of the cylinders. When an infinitely long cylinder is perpendicularly illuminated, light is scattered only in the plane which is perpendicular to the cylinder axis.

The simulations were compared to goniometric measurements on soft wood (*picea abies*) which are presented in Fig. 5c. An excellent agreement was obtained between the measurements and the simulations without adjusting any parameter in the model used in our earlier publication besides the assumption of a small gaussian distribution of the cylinders' (the tracheids') directions of 1° along the x -axis.

4. Discussion and conclusion

In summary, we have demonstrated that for the following three criteria a Lambert surface does indeed exist: a) the albedo $a = \mu_s / (\mu_s + \mu_a)$ equals 1, b) the refractive index is the same inside and outside the turbid medium, c) the angular dependence of the incident light power is $\propto \cos(\theta)$.

In our investigations we assumed that the turbid media have a plane surface. We note that we programmed several models (e.g. a ray tracing method) for calculation of the angular reflectance of rough surfaces [19, 20] and found that due to self-shadowing there is a decrease of the emitted light at polar angles close to 90° which rules out the possibility of obtaining the exact Lambert law for media with rough surfaces.

The calculations shown were based on radiative transfer theory. This theory, although being abundantly applied, is an approximation of the Maxwell equations which accurately describe the interaction of light and matter within the framework of classical physics [21, 22]. Recently, we compared solutions of the radiative transfer equation with analytical solutions of the Maxwell equations and found that radiative transfer theory correctly describes the light propagation for relatively low scatterer concentrations (e.g. < 20 vol% for polystyrene spheres with a diameter of $2\ \mu\text{m}$) with the exception of interference effects like speckles or coherent back scattering [23]. The latter can be avoided by using a light source with infinitely small spatial extension, because practically no coherent time-reversed scattering paths interference can occur. Both effects can be excluded by using a light source with a low coherence length. Thus, a Lambert surface can, in principle, even be derived by applying Maxwell equations.

It was shown, by using other optical and geometrical conditions than the three listed above, that there is always a systematic deviation from the Lambert surface. This is also the case when these conditions are fulfilled but the spatially resolved or time resolved reflectance and not the total reflectance is considered.

In addition, a huge deviation from the Lambert law was found when not only the dependence on the polar angle but also on the azimuthal angle was examined at a certain position relative to the incident beam. This non-Lambertian characteristic of the reflectance is even found at large distances. Beside its importance, the dependence on the azimuthal angle has been neglected for many applications so far.

We calculated the angular resolved reflectance from wood representing the relevant class of turbid media that exhibit an anisotropic light propagation. Even for the total reflectance we found a large deviation from the Lambert law which was in close agreement with goniometric measurements. The angular (both polar and azimuthal) dependence of the reflectance on the aligned microstructure of the tissue is predestined for early detection of tissue alterations.

The combination of all the different possibilities, e.g. $R(\theta, \phi)$ is examined at a certain location and a certain time after the irradiation of a $\delta(t, r)$ -source (having a certain incident direction) onto a turbid medium with aligned microstructure, delivers even more involved reflectance

characteristics. Further, for the above presented results unpolarized light was assumed. Implementation of light propagation of polarized light gives additional features which can be used for investigation of the microstructure of turbid media. Therefore, 250 years after Johann Heinrich Lambert published his famous law the investigation of the angular light reflectance from turbid media is a more vivid research field than ever before.